Article

The Use of Double-Skin Façades to Improve the Energy Consumption of High-Rise Office Buildings in a Mediterranean Climate (Csa)

Atef Ahriz [1,*], Abdelhakim Mesloub [2], Leila Djeffal [1], Badr M. Alsolami [3], Aritra Ghosh [4,*] and Mohamed Hssan Hassan Abdelhafez [2,5]

[1] Department of Architecture, University of Tebessa, Constantine Road, Tebessa 12000, Algeria; ledjeffal@gmail.com

[2] Department of Architectural Engineering, College of Engineering, University of Hail, Hail 2240, Saudi Arabia; a.maslub@uoh.edu.sa (A.M.); mo.Abdelhafez@uoh.edu.sa (M.H.H.A.)

[3] Faculty of Islamic Architecture, College of Engineering and Islamic Architecture, Umm-Al-Qura University, P.O. Box 715, Makkah Al Mukarramah 21955, Saudi Arabia; bmsolami@uqu.edu.sa

[4] College of Engineering, Mathematics and Physical Sciences, Renewable Energy, University of Exeter, Exeter TR10 9FE, UK

[5] Department of Architectural Engineering, Faculty of Engineering, Aswan University, Aswan 81542, Egypt

* Correspondence: atahriz@gmail.com (A.A.); a.ghosh@exeter.ac.uk (A.G.)

Abstract: Engineers use double-skin façades (DSF) to lower the energy consumption of buildings as they can potentially control incoming wind speeds and the amount of solar heat gain. The purpose of this present study was to (1) evaluate the use of DSFs, (2) its efficacy in improving the energy performance of high-rise office buildings in the hot, dry summer climate of the Mediterranean, and (3) to develop an optimum DSF model for this climate based on industry standards and recommendations for high-performance DSF parameters. In order to determine the efficiency of DSFs, two distinct variables, building orientation and the number of DSFs used, were taken into consideration. This study adopted an experimental (generate and test) research design and used Autodesk® Ecotect® Analysis software to develop computer simulations with which to assess 15 single façades, juxtaposed façades, three façades, and four façades on cardinal orientations. The recorded energy consumption and savings were then compared with that of the reference model. The results indicated that the three DSF model, i.e., the S14 model, reduced energy consumption during heating by 28% and by 53.5% when cooling a high-rise office building located in the hot, dry summer climate of the Mediterranean (Csa).

Keywords: double skin façade (DSF); energy saving; heating; cooling; Mediterranean climate; high-rise building

1. Introduction

In the twentieth century, glass has not only become an essential architectural feature but one of the primary elements that determine the extent to which the structure affects the aesthetics of space as well as the psychology of its occupants [1]. The idea of transparency has become crucial in architectural design the world over as it emphasizes communication between the internal and external surroundings of a building as well as maximizes solar energy benefits while increasing natural illumination [2]. However, due to the effects of global warming in recent years, engineers and architects have observed that glass has become detrimental to the energy consumption of a building as the air that has been preheated by direct solar radiation and atmospheric temperature infiltrates a space through the glass, thereby, increasing the cooling requirements of a building and bucking the trend. Therefore, in order to address these issues as well as manage weather conditions without completely abandoning the use of glass in buildings, several solutions and techniques; such as solar

screens [3], double or triple glazing [4], advanced smart switchable glazing [5,6] changing the type of glass and its composition [7], Semi-Transparent Photovoltaic (STPV) [8,9] and double-skin façades (DSFs) [10,11]; have been developed.

The latter of which is the most reliable solution as it is capable of controlling the speed of incoming winds, regulating the solar heat gain of buildings, and reducing noise pollution in noisy cities. The mechanism of action of DSFs relies on the creation of an air corridor or an air cavity between two layers of glazing on a façade that prevents temperate air from entering the building by dispelling it to the exterior in the case of a hot climate [12–14].

However, the high performance and efficiency of DSFs depend on several factors; such as the configuration of the double-skin façade [15–17], i.e., box windows, shaft boxes, corridors, or multi-story façades, the origin of the air flow, i.e., supply air, exhaust air, buffer zones, or outdoor or indoor air curtains, the parameters of the building site, i.e., orientation, solar irradiation, and wind conditions, the use of natural or mechanical ventilation, the width of the air cavity, the use of shading devices, and material composition. Architects have successfully applied these highly efficient solutions in a variety of buildings in differing global climates, including the 30 St Mary Axe office building (informally known as the Gherkin) built by Foster + Partners in 2001 in the temperate and mild oceanic climate of London, the Kraanspoor office building in Amsterdam built by OTH architecten, and the Sendai Mediatheque by Toyo Ito in 2001 in the hot and humid continental summer climate of Japan [14].

The Mediterranean climate is a temperate climate found in the Mediterranean basin, from California to the United States of America, South Africa, and South Australia. It is characterized as having abundant sunshine, hot and dry summers ranging between 25 °C and 40 °C, mild and humid winters averaging 5 °C, and rain in the intermediate seasons [18].

In recent years, Algeria has launched development and improvement strategies that will usher the country into a new era. One such strategy is the development of the Bay of Algiers. A component of the country's Strategic Plan for Vision 2030, it aims to provide the capital with a new image and create a new seafront. It also aims to achieve attractiveness, sustainability, and use less energy. Therefore, the following questions were posed:

Which DSF configuration provides the most optimal energy performance in high-rise office buildings in the Mediterranean climate of Algiers City?

Which parameters of the chosen DSF affect efficiency and reliability as well as improve the energy performance of office buildings in Mediterranean climates?

Tests of different models and their variables in different climates indicate that multi-story DSFs could potentially improve the energy performance of high-rise office buildings in Mediterranean climates. However, the orientation and number of DSFs used on the various façades of a high-rise office building affect its energy performance and energy efficiency. As such, the purpose of this present study was to determine the reliability of multi-story DSFs and the effect of two variables on the energy performance of DSFs in high-rise buildings in the Mediterranean climate of Algiers City.

2. Literature Review of Double-Skin Façade Systems

The use of DSFs became a trend in European architecture as it preserves transparency as well as enhances interior–exterior communication by facilitating better natural lighting, acoustic and thermal comfort, protection from extreme weather conditions, and, therefore, less energy consumption [12,13]. According to Yellamraju (2004), DSFs are classified based on their configurations and air flow through the cavity (Figure 1). As such, several classifications have been developed to provide researchers and designers with additional details that maximize DSF utilization [19]. As reported by Poirazis (2004), the Belgian Building Research Institute (BBRI) proposed a more detailed method of classifying DSFs in 2002. This included details, such as the type of ventilation, the source of the airflow, the destination of the airflow, the direction of the airflow, the cavity width, and the type of partitioning [13]. However, Saelens (2002) classifies DSFs according to primary characteristics that describe and facilitate the understanding of the mode of operation and creation of the DSFs, the

origin of the air flow, the driving force of the air flow, and the compartmentalization of the façade [20]. The origin of the air flow is considered the most critical parameter in a DSF as it has a significant effect on the average temperature of the cavity. Supply air, exhaust air, interior and exterior air curtains, and buffer zones are air flow concepts that represent the ventilation modes of cavities [20,21].
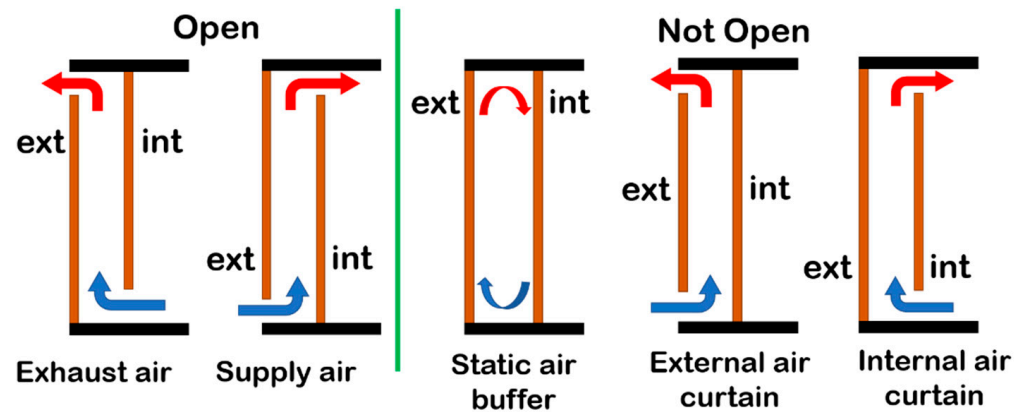

Figure 1. The ventilation modes of cavities (author).

As the driving force of an air flow may be natural or mechanical, understanding it dictates the continuity and controllability of the air flow [20,21]. Façades can be categorized into four distinct DSF designs: (1) a multi-story façade, (2) a shaft box, (3) a corridor, or (4) a box (Figure 2) [20–23].
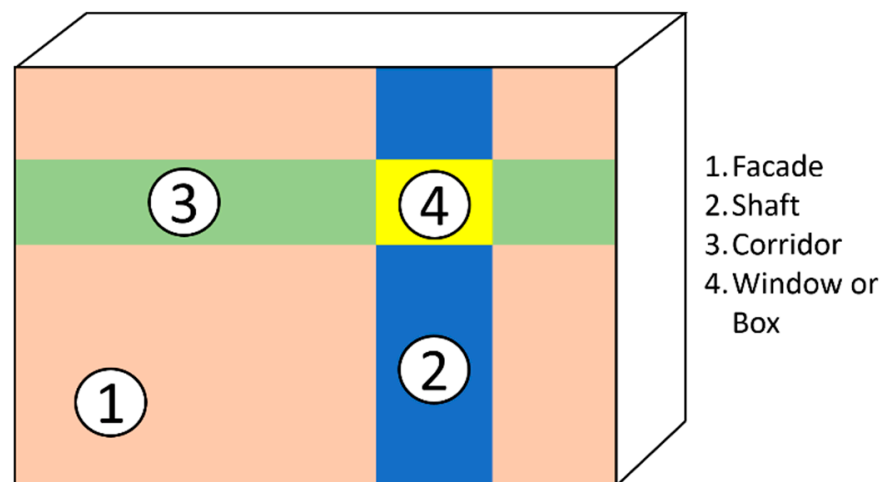

Figure 2. Types of DSFs based on compartmentalization designs.

Furthermore, DSF performance depends on the design, site, and building parameters. Firstly, the design takes into consideration the general characteristics of a DSF. This includes the cavity width, the shading devices used, the glazing properties, and the compartmentalization of the façade, as illustrated above [20,23,24]. Secondly, DSF performance is affected by the parameters of a building. This includes technical characteristics, such as height or floor count, the materials of the inner layer of the façade, and the location and size of the openings on the inner layer of the DSF [23]. Lastly, DSF performance is affected by the parameters of the site as it is dependent on the external parameters of the surrounding site. This includes solar irradiation, orientation, external temperature, wind speed, and wind direction [23].

2.1. Double-Skin Façade Operating Modes

A DSF operates differently during cooling and heating periods: in hot climates, heat accumulates in the cavity and is partially transferred to the adjacent space via air that is introduced through the cavity openings. This excess heat is moved to the exterior of a building via the stack effect. In the stack effect, differences in air density create a circular flow that releases hotter air, thereby lowering the temperature of the inner layer of the DSF and reducing the amount of heat that is transferred into the interior space. When sunscreens are sandwiched between two layers of a DSF, they either absorb or reflect harmful solar radiation. In conclusion, as the temperature in the air cavity rises, the air is expelled, creating a light breeze and mitigating heat gain, thereby decreasing the cooling demand of the occupied space.

Although air cavities act as a barrier and insulator against heat loss in cold climates, thereby reducing the demand for indoor heating systems, there are two reasons why heating is required. The first reason is a lack of air circulation within the closed cavity. As the air is heated by the sun, it raises the temperature of the interior glazing of the DSF. This results in conductive, convective, and radiant losses within the space. The second method involves introducing air into the cavity from the inside to heat the inner skin and achieve the same result. The air is then routed to the building system and passed through a heat exchanger to preheat the incoming air (Figure 3) [19,25].
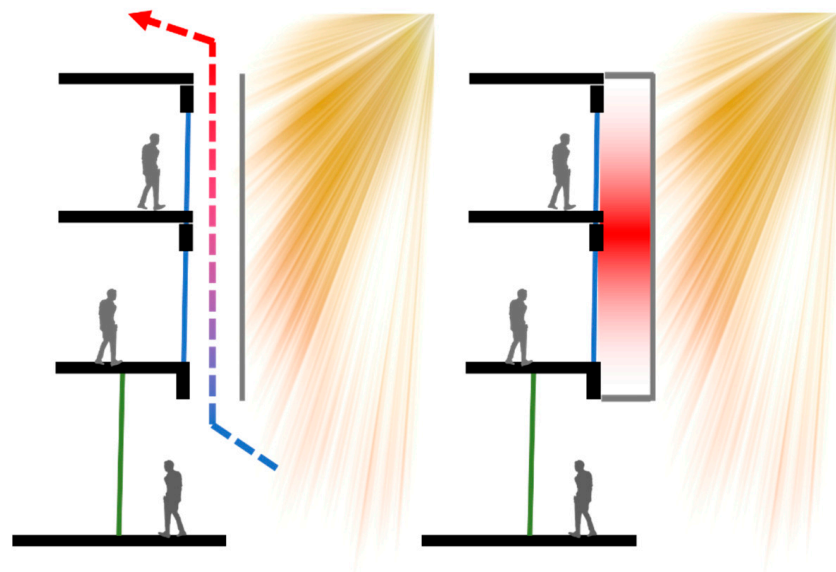

Figure 3. The operating modes of DSFs in hot and cold climates (author).

2.2. Literature Review of Double-Skin Façades

Based on the data collected from past studies and experiments that evaluated the energy performance of DSFs in high-rise buildings in various climates (Table 1), the various DSF parameters were analyzed and correlated with the expected results. This present study aimed to develop a DSF model using parameters that have been proven to affect the energy consumption performance of DSFs in high-rise buildings as well as to test the model using the co-efficient of performance. Each of the studies reviewed followed a four-step structure: (1) the variables used in the experiment, (2) the simulation model used in the experiment, (3) the type of ventilation chosen, and (4) the main findings of the study. These findings were used to conduct a robust experiment of the case study in order to accomplish the objectives of this present study.

Table 1. Studies on the Building and site design parameters of the double skin façade.

The Experiment	Parameters of the Experiment		Main Findings
Yoon, N., et al., 2022 Korea, Seoul. Ref. [26]	Variables	cavity height, cavity depth, opening-to-glazing ratio, (SHGC)	• When the cavity height was increased, the increased cavity depth combined with a higher opening glazing ratio aided in the process. • Although a higher SHGC increased airflow, it also increased the room temperature.
	Tools	CFD	
	Ventilation type	Natural ventilation	
Hong, X., et al., 2022. China. Ref. [27]	Variables	roller shades, Blinds, daylight and thermal performances	• Integration of DSF with a multisectional shading system and appropriate control algorithms can result in annual energy savings of up to 6.8 percent and 4.8 percent for buildings in Xiamen and Shanghai, respectively.
	Tools	Energy-plus, Radiance	
	Ventilation type	Air conditioned	
Radhi et al., 2013 Al-Ain city, UAE. Ref. [28]	Variables	The width of the cavity: 50, 70, 100, 120, 150 cm	• The heat transfer rates decrease when the width of the cavity is reduced due to the high ventilation rates. • The width of the cavity between 0.7 and 1.2 m can provide a balance between solar gain and heat transfer.
	Tools	Design-Builder (BES) + PHONICES-FLAIR (CFD)	
	Ventilation type	Air conditioned	
Chan et al., 2009 Hong Kong, China. Ref. [29]	Variables	Type of glazing: single and double	• The inner layer in simple transparent glass + Low transmissivity double glazed outer layer can reduce the heat gain and cooling energy of the building.
	Tools	Energy Plus (BES)	
	Ventilation type	Air conditioned	
Guardo et al., 2009 Barcelone, Belgique [30]	Variables	Glass transmissivity (from 35 to 78%) and emissivity (from 0.05 to 0.89)	• Replacing the internal glazing with low-emissivity glass can reproduce the reduction in solar charge gain. • The reduction of the transmissivity of the external glazing can play a role in reducing the solar charge gain from 55% to 40%.
	Tools	CFD	
	Ventilation type	Air conditioned	
Section 2: studies on DSF building parameters			
Haase et al., 2009 Hong Kong, China. Ref. [31]	Variables	The window-wall ratio: 63, 91.32%	• The WWR type and the type of glazing have a great influence on the annual cooling load. • The DSF system with a large internal window (Window to Wall ratio WWR = 0.91) has the same annual cooling load as the singl© facade system with a small window area (WWR = 0, 32).
	Tools	TRNSYS and TRNFLOW (coupled with COMIS)	
	Ventilation type	Mechanically ventilated cavity	
Tao, Y., et al., 2021 [32]	Variables	Dimensions of DSF, Size of window openings; Gap depth	• The optimal vent height is should be around 0.2–0.3 m • Sidewall windows are found to provide superior indoor airflow coverage. • Window placement and room dimensions have a minor effect on ventilation rates.
	Tools	CFD software ANSYS Fluent 2020R1	
	Ventilation type	Natural ventilation	
Pappas and Zhai 2008 Belgiqueles, Belgique [33]	Variables	The height of the cavity/Number of floors: 3.0 m (one floor) and 15.0 m (5 floors)	• A taller cavity will produce a stronger buoyancy effect, creating a larger air flow.
	Tools	Energy Plus (BES) + PHONICS (CFD)	
	Ventilation type	Not mentioned	
Section 3: Studies on DSF site and climate condition parameters			
Yoon, Y.B., et al., 2020 South Korea [34]	Variables	-Cold climate	• The results reveal that the apartment with the DSF retrofit saves 38.8% on the annual heating energy compared to existing balcony windows
		-Heating energy savings	
	Tools	-The EnergyPlus	
	Ventilation type	-Air conditioned	
Gratia and DeHerde 2007 Uccle, Belgium [35]	Variables	-Clear and medium cloudy conditions -Orientations East and West	• On sunny days, the temperature in the cavity of the double-skinned facade facing south has exceeded room temperature by about 20 °C. However, under cloudy sky conditions, the maximum temperature difference from the outside temperature was 10 °C
	Tools	TRNSYS and TRNFLOW (coupled with COMIS)	
	Ventilation type	Mechanically ventilated cavity	

Table 1. *Cont.*

The Experiment	Parameters of the Experiment		Main Findings
Shakouri, M., et al., 2020 middle eastern region [36]	Variables	-Hot climate -Building integrated photovoltaic thermal double skin façade	• The building integrated photovoltaic thermal double skin façade system has the potentiality of dropping the annual cooling and thermal loads significantly.
	Tools	MATLAB software	
		PVsyst software	
	Ventilation type	Naturel ventilation	
		Air conditioned	

3. Research Methodology

This present study combined two of the most valuable approaches in building modeling and simulation tools: (a) process-based simulation and (b) sensitivity analysis. According to Ahriz (2021), sensitivity analysis in building performance analysis relies on two approaches: (a) global sensitivity analysis and (b) local sensitivity analysis [37]. Local sensitivity analysis relies on the one-factor-at-a-time (OVAT) method by Chaudhry and Buchwald [38], while the process-based simulation is compatible with the OVAT method. The sensitivity is determined when one variable is modified while the other parameters remain constant [39]. Therefore, this present study employed local sensitivity analysis because it is:

- Straightforward in its application and interpretation,
- Much simpler to use than global sensitivity analysis, and
- Based on the OVAT approach, which is the same technology used in process-based simulations to generate and test the techniques.

Sensitivity analysis utilizes the same methodology as process-based simulations. It begins by determining variations in the input parameters. A model is then created based on the architectural model before it is simulated. The results of the simulation are then subjected to a sensitivity analysis [39]. All of these phases were taken into account in this present study, from the method selection through to the rigorous sensitivity analysis of the discomfort index for three distinct periods: (1) hot, (2) cold, and (3) global.

The experiments conducted in this present study used the OVAT method in conjunction with the process-based simulation. Autodesk® Ecotect® Analysis software was used to simulate the climatic behavior of the DSF according to five parameters: (a) the structure of the DSF, (b) the cavity width, (c) the type of glazing, (d) the opening dimensions of the cavity, and (d) the type of ventilation. Three basic steps were required to accomplish this goal. Firstly, the hypothetical basic model was identified while all the variables of DSF to be tested were outlined. A digital simulation was then conducted to produce results. Lastly, the energy loads results were interpreted and analyzed to determine the impact of the selected DSF scenario parameters and to highlight general recommendations (Figure 4).
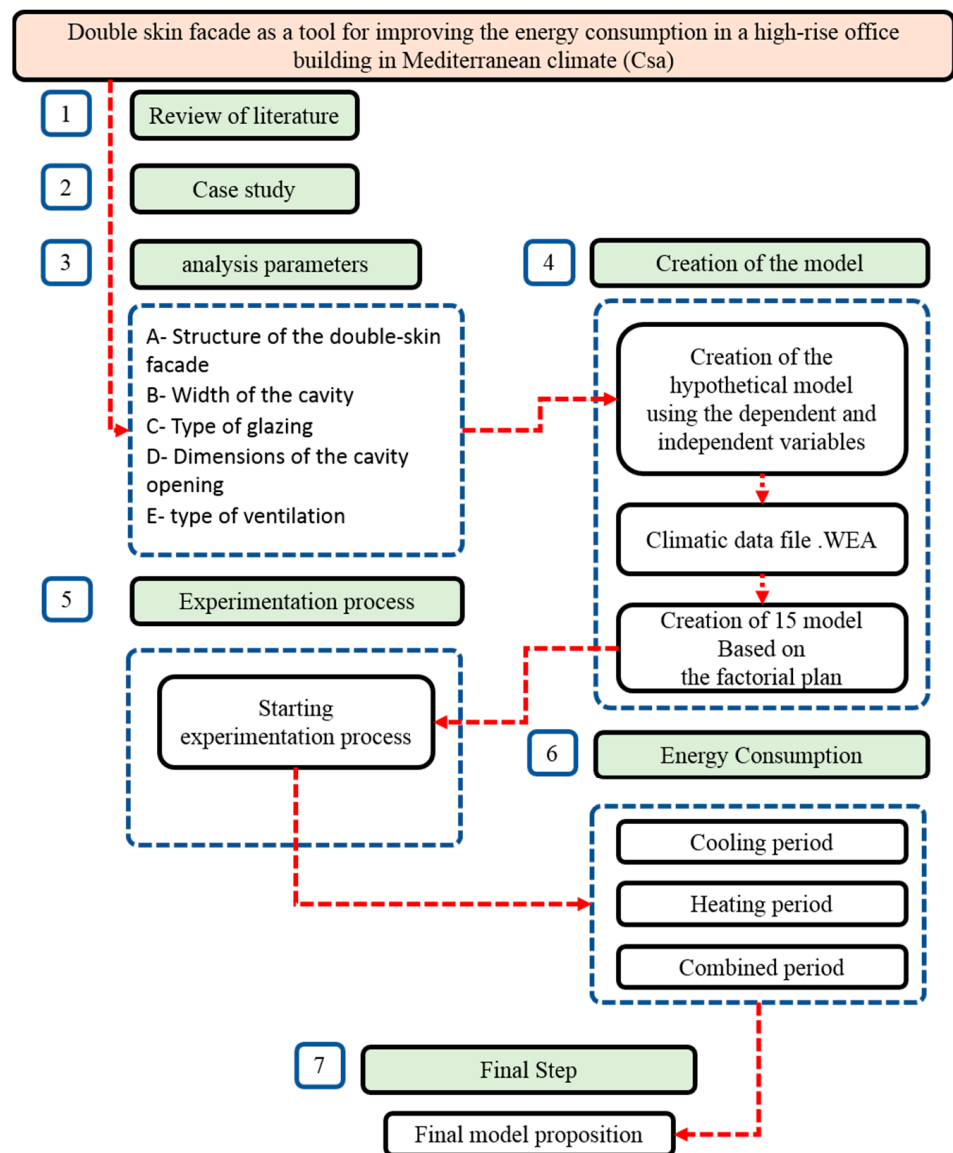
Figure 4. Conceptual framework of this present study.

4. Case Study

4.1. Environment

The capital of Algeria, Algiers City, was chosen as the case study model of a Mediterranean climate. Algiers City is situated in the extreme north of Algeria and on the south coast of the Mediterranean Sea at 36°45′14″ N 3°3′32″ E [40]. It has a Mediterranean climate [41] (Köppen climate classification Csa) with a hot dry summer [41]. According to the global meteorological database, Meteonorm [42], August is the warmest month of the year, with an average temperature of 26.2 °C, while January is the coldest month of the year, with an average temperature of 10.1 °C [43]. The wind blows mostly from the east for 4.7 months between May to October and from the west for 7.3 months between October to May. The windiest period of the year is between the 29th of October and the 16th of April (5.6 months), with an average wind speed of about 15.0 km/h [44] (Figures 5 and 6).
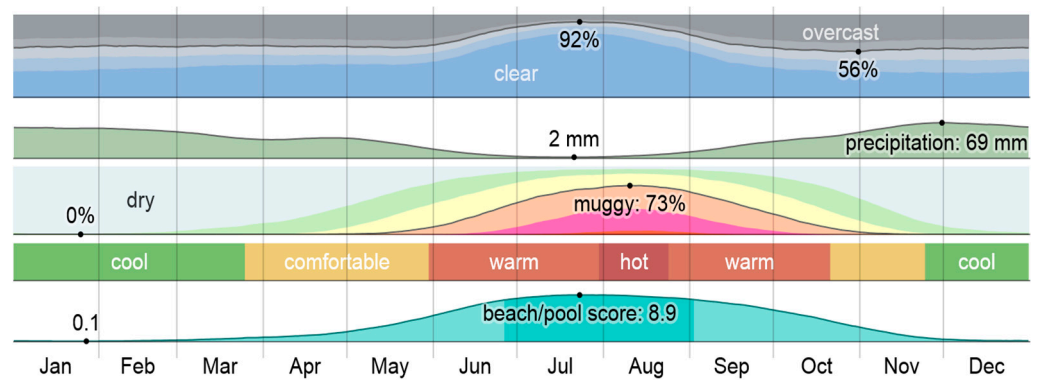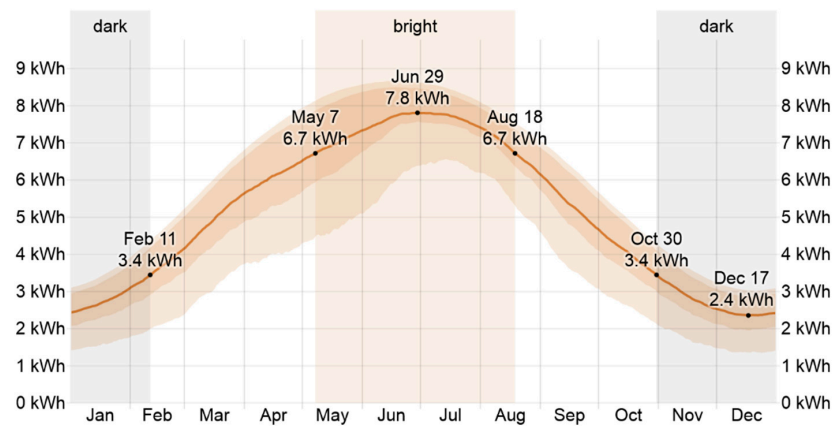
Figure 5. Climate of Algiers City [44].

Figure 6. Average daily incident shortwave solar energy in Algiers City [44].

The average daily incident of shortwave solar energy varies significantly according to the seasons of the year. The bright period lasts for 3.4 months between the 7th of May and the 18th of August, with an average daily incident shortwave energy per square meter that exceeds 6.7 kWh. July is the brightest month of the year, with an average of 7.7 kWh. The dark period lasts for 3.4 months between the 30th of October and the 11th of February, with an average daily incident shortwave energy per square meter below 3.4 kWh. December is the darkest month of the year, with an average of 2.4 kWh [44] (Figure 7).

Figure 7. A 3D models of the case study.

4.2. Building

The purpose of this present study was to apply bioclimatic architecture principles in the design of a new multifunctional center in Algiers City. The primary aim of this design was the development of an environmentally-friendly building with optimal energy performance. To that end, a DSF technique was developed to enhance the energy performance of the entire building. The building consisted of two parts: (1) a horizontal bar with three levels and (2) a tower with 32 levels where the DSFs were tested according to several parameters.

5. Analysis Model Development

An analysis model was created in two steps. The first step involved determining the three detailed parameters of the building: (1) the site, (2) the building, and (3) the DSF parameters (Table 2). The second step involved determining the dependent and independent variables of the model (Table 3). Based on the factorial plan theory, the proposed model was then divided into 15 different scenarios according to the orientations and positions of the DSF (Table 4).

Table 2. Parameters of the analyzed model.

Site parameters	Csa Mediterranean Climate determined with a detailed WEA climatic data-set file extracted from Meteonorm tool
Building parameters	Total height of the analyzed building is 36 m, with 9 floors of 4 m.
	Interior layer of the DSF is a single glazing with U-value = 6 W/m^{2}K.
	DSF is multi story structure type and the building is with a complete HVAC system, therefore the inner facade is completely transparent without openings.
DSF design parameters	The width of the cavity: 0.90 m
	Shading devices: None
	Outer skin with a low double-glazing emissivity: 0.10 with a U-value = 2.4 W/m^{2}K, SHGC = 0.56
	Type of ventilation: Natural

Table 3. Variable of the Simulation process.

Independent variables	*Fixed independent variables*	Structure of the DSF	Structure type of the DSF is multi story, with 9 floors and 36 m height.
		Width of the cavity	The width of the cavity is wide = 0.9 m.
		Type of glazing	• Glazing properties of the outer skin is a double low emissivity glazing with U-value 2.4 W/m^{2}K. • Glazing properties of the inner skin is a single glazing with U-value 6 W/m^{2}K.
		Dimension of the cavity opening	The cavity have an external air curtain based on two openings having the same dimensions of the cavity it self.
		Type of ventilation	Natural ventilation.
	Non-fixed independent variables	Orientation	Proposed orientations of the DSF are: North, South, East, West.
		Number and position of the tested DSF's	Proposed scenarios of the DSF: • Single façade. • Two opposing DSFs. • Two juxtaposed DSFs. • Three DSFs. • Four DSFs.
Dependent variables	• Energy consumption during heating period (KWh). • Energy consumption during cooling period (KWh).		

Table 4. Different scenarios of the simulation process basing on the factorial plan theory.

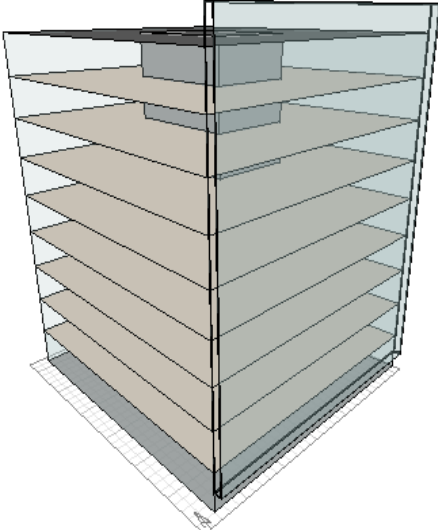|			
No DSF Used			
Orientation	///		
Scenario code	S00		
Single DSF			
Orientation	S	N	E	W
Scenario code	S01	S02	S03	S04
Two Opposed DSFs			
Orientation	N + S		E + W	
Scenario code	S05		S06	
Two Juxtaposed DSFs			
Orientation	S + E	E + N	N + W	W + S
Scenario code	S07	S08	S09	S10
Three DSFs			
Orientation	S + E + N	E + N + W	N + W + S	W + S + E
Scenario code	S11	S12	S13	S14
Four DSFs			
Orientation	E + N + W + S			
Scenario code	S15			

6. Modelling and Simulation Process

Among several energy simulation tools available, Autodesk® Ecotect® Analysis software has been used and validated by multiple studies [37,45–51]. Ecotect was chosen for this study due to its ability to help architects with the design decision-making step in a large list of parameters as well as thermal comfort, energy performance, acoustic levels, lighting, and air movement. In this research, a building energy simulation was made based on the Chartered Institute of Building Services Engineers (CIBSE) Admittance Method; its algorithm is very flexible and has no restrictions on building geometry or the number of thermal zones that can be simultaneously analyzed.

Among the different thermal simulation engines available is the CheeNATH engine from CSIRO in Australia based on the response factor method, the DOE2 (now EnergyPlus) from the US based on ASHRAE methods, and the TAS (Thermal Analysis Software) by EDSL in Britain. The Admittance Method is widely used around the world and has been shown to be an extremely useful design tool. It is not as physically accurate as some of the more computationally intensive techniques such as the response factor or finite difference methods. However, for the purposes of design decision-making, the Admittance Method is by far the best choice.

The model was a geometric abstraction of a high-rise office building. The polyhedral section was 36 m^2 in height, while the story section was 852 m^2 in floor area. The main function of the building was an open-type office with roughly 74 occupants, working six days a week between 8 a.m. to 7 p.m. with 60 w as an average biological heat output according to reading/writing activities and 1.0 Clo as light business suit clothes. The lighting level was predefined at 400 Lux, which is suitable for office desk work. The model assumed maximum energy consumption with a full HVAC system throughout the year, with a dual-duct variable air volume (VAV) system. The comfort level selected for the simulation ranged from 18 °C to 26 °C. The DSF cavity was 0.9 m and ventilated naturally, while the outer skin was made of a low double-glazing with an emissivity of 0.10, a U-value of 2.4 W/m^{2}K, and an SHGC of 0.56 (Tables 2, 3 and 5). A total of 16 different scenarios with varying numbers of DSFs and orientations were simulated. This included Scenario S00, which was the reference case study without the use of a DSF (Table 4).

Table 5. Model Parameters and inputs for DSF.

Building	Details	3D Model Building Simulation
Building type	High-rise office	
Office type	Open office	
Characteristics	**Value**	
working hours	08 a.m.–19 p.m.	
N° Occupants	74	
Clothing index	1.0 Clo	
Biological heat output	60 w	
N° storey	09	
Area	858 m^2	
Storey Height	04.00 m	
Comfort temperature	18 °C–26 °C	
Humidity	60%	
Sensible gain	05 W/m^2	
Latent gain	02 W/m^2	
Air change rate	0.5 ach	
Wind sensitivity	0.25 ach	
Light level	400 Lux	
HVAC (full AC)	Dual duct VAV	
Thermal simulation engine	Admitance method	
CORE engine	CIBSE	
Glazing Type	**Multi-story**	
Single glazing 6 mm	U-value 6 Wm^2/k	
Double glazzing 4 mm	U-value 2.4 Wm^2/k	

7. Results and Discussion

The results of the 15 DSF scenarios, which were set up in several cardinal orientations in a Mediterranean climate, were numerically investigated in terms of energy consumption. The results provided the seasonal and annual consumption curves of each scenario.

7.1. Monthly Energy Consumption during Heating Period

As seen in Figure 8, the energy consumption for heating during winter was recorded for six months between November to April. The line graph of each scenario was classified into four groups. The first group comprised only Scenario S15, where the annual energy of the building did not exceed 2000 KWh due to the quadruple protection of the DSFs used. The second group contained Scenarios S09, S12, and S13. As seen in the graphs, the energy consumption ranged between 8000 KWh to 11,000 KWh in January and did not surpass 5000 KWh in December. Triple protection ranked second to the double DSF used in the north and south façades, as the energy gained from the south façade was high. The third group comprised Scenarios S0, S02, S04, S05, S06, S08, S10, S11, and S14, where the energy consumption varied between 12,000 KWh to 16,000 KWh in January and 4000 KWh to 8000 KWh in December. Lastly, the fourth group contained Scenarios S01, S03, and S07, which consumed the most energy. The energy consumed in January ranged between 17,000 KWh to 19,000 KWh and was 12,000 KWh in December. These three scenarios consumed the most energy as DSFs were used in the south and/or east of the façade. This can be explained by a loss of energy from the coolest façade, which was the north and/or west.
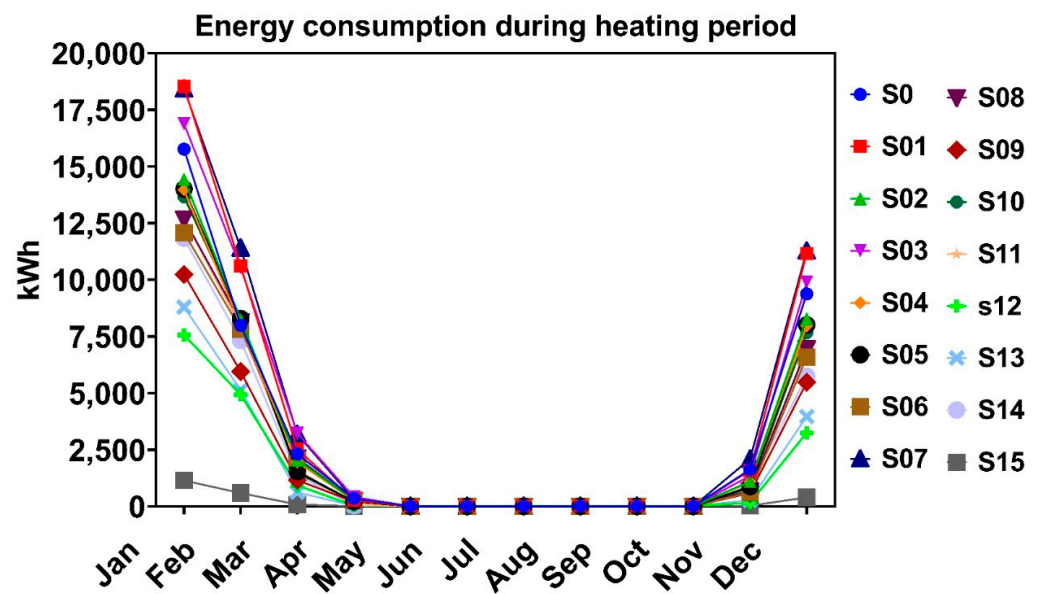
Figure 8. Energy consumption during heating periods in KWh.

7.2. Monthly Energy Consumption during Cooling Period

As seen in Figure 9, the energy consumption for cooling during the summer was recorded for 10 months between February to November. The line graph of each scenario was classified into five groups. The first group contained only Scenario S14, where the energy consumption of the building did not exceed 7000 KWh in August. Although the amount of energy required for cooling was reduced, it was still required for seven months between April to October. This was due to the triple protection of the DSFs used in the south, east, and west façades, which are the worst performing façades in a Csa climate. This is because a building can lose the extra energy that it has gained via the north façade during the summer. The second group comprised S01, S03, and S04. The graphs showed that the energy consumption ranged between 8000 KWh in July and 1000 KWh in August and that cooling was still required for eight months between March to October. Single protection ranked second in this instance as the south, east, and west façades are the worst performing façades in the summer, while the north façade remains cool due to low exposure to solar radiation. The third group contained Scenarios S05, S06, S07, S08, S09, S10, S11, S12, and S13, where the energy consumption reached the upper limit of 12,000 KWh in August. A total of 90% of the scenarios studied in this group used double DSFs. This phenomenon could be explained by the creation of a local greenhouse effect in the cavity as the high energy received and the low ventilation in the cavity provides the DSFs with few opportunities to cool over the nine-month period between March to November. The fourth group comprised only Scenario S02, where the energy consumption exceeded 12,000 KWh. This was due to the exposure of the south, east, and west façades to solar radiation, while only the north façade, the coolest, was equipped with DSFs in the summer. The last group comprised Scenario S00, which was the reference case study. As it was not equipped with any DSFs, the energy consumption approached 14,000 KWh, and cooling was required for 10 months of the year.
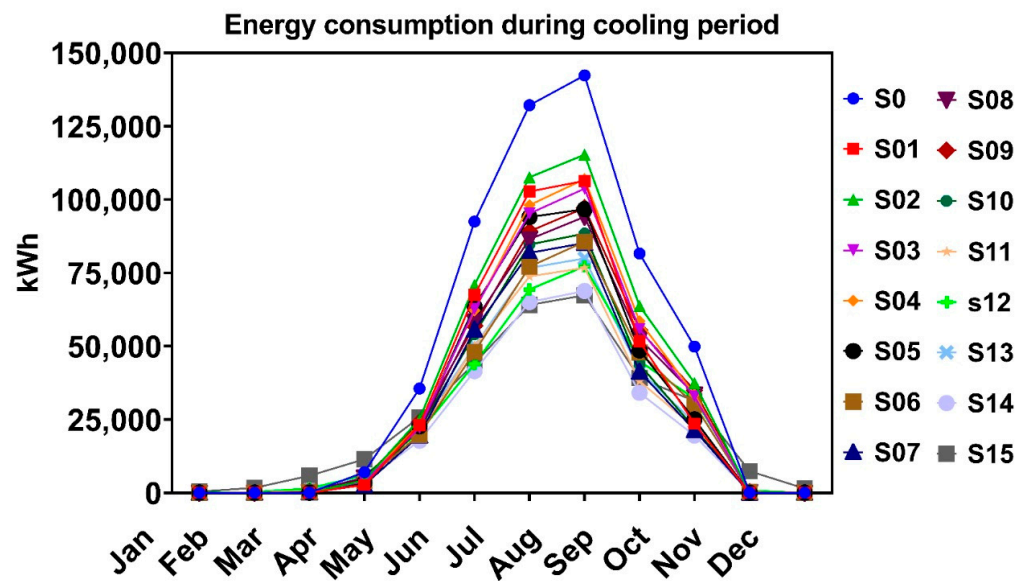
Figure 9. Energy consumption during cooling periods in KWh.

7.3. Overall Energy Consumption and Energy Savings

7.3.1. Annual Energy Consumption during Heating Period

The total energy consumption of the 16 different scenarios during the heating period was analyzed. As seen in Table 6 and Figure 10, the minimum annual energy consumption was 2217 kWh in Scenario S15 as it used four DSFs, while the maximum annual energy consumption was 46,677 kWh in Scenario S07, which used two juxtaposed DSFs on the south and east façades.
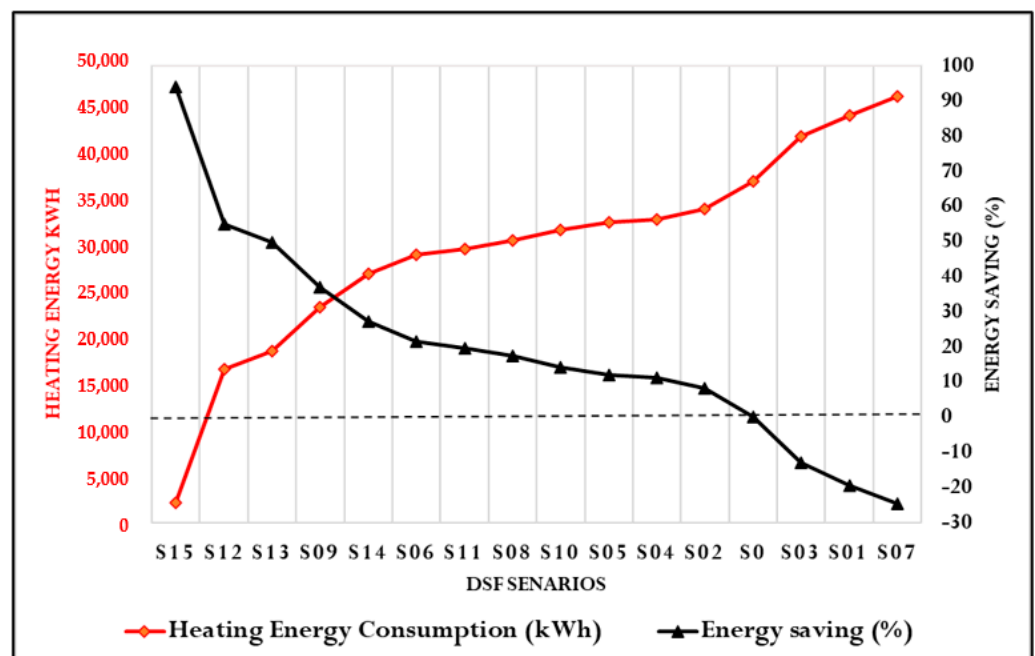
Figure 10. Classification of the scenarios according to energy consumption during heating periods.

According to Tables 6 and 7 and Figure 10, Scenario S15 had the most efficient energy consumption during heating periods as it used four DSFs on all façades. This resulted in energy savings of approximately 44,459 kWh due to the generation of a local greenhouse effect within the cavity surrounding the building, where the interior skin helped maintain the temperature within the building and the DSFs provided an insulating effect. In Scenario

S12, three DSFs were mounted on the east, north, and west façades resulting in energy savings of 27,883 kWh, while, in Scenario S13, three DSFs were mounted on the north, west, and south façades resulting in energy savings of 29,840 kWh. This was due to the greenhouse effect as well. However, the energy consumption increased due to energy loss via the fourth unprotected façade.

The amount of energy loss prevented in the cavity of the DSFs increased when two juxtaposed or opposite DSFs were used. The average energy savings of the two orientations varied between 12,314 kWh and 19,471 kWh. The use of only one DSF or two juxtaposed DSFs were found to accelerate energy loss from the cavity and the interior. This was because the heat gained within the cavity was expelled to the exterior via the stack effect. This reduced the amount of heat transferred to the interior, thereby increasing the amount of energy required to heat the interior of the building.

7.3.2. Annual Energy Consumption during Cooling Period

The total energy consumption of the 16 different scenarios during the cooling period was analyzed. As seen in Table 6 and Figure 11, the minimum annual energy consumption was 30,031 kWh in Scenario S14 as it used three DSFs, while the maximum annual energy consumption was 540,919 kWh in Scenario S00, which did not use any DSFs.
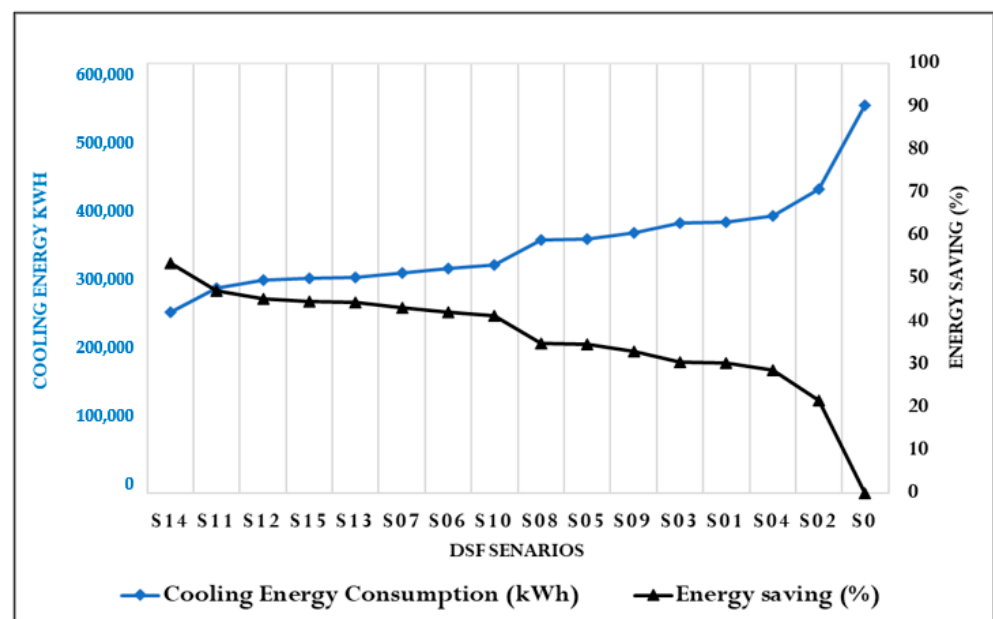

Figure 11. Classification of the scenarios according to energy consumption during the cooling periods.

As seen in Tables 6 and 7 and Figure 11, Scenario S14 had the most efficient energy consumption as it used three DSFs on the east, south, and west façades. This resulted in energy savings reaching 289,074 kWh due to the attenuation of the amount of solar heat transferred, which correlates directly with the solar geometry of the studied region. Furthermore, when the temperature of the air within the cavity increased, the slight inflow of outdoor air via the openings of the cavity evacuated this excess heat outside the building through the stack effect. This helped decrease the cooling demand of the interior space. Scenarios S11, S12, and S13, which used three DSFs, also yielded significant energy savings of between 239,896 kWh and 254,633 kWh but fewer energy savings than Scenario S14. This was due to the heat gained via the exposure of the unprotected façade to direct solar radiation, which increased the cooling demand. A new phenomenon was discovered in Scenario S15, which used four DSFs, which was the generation of a local greenhouse effect in the north façade.

The amount of energy loss prevented in the building, and the DSF increased when two juxtaposed or opposite DSFs were used. The average energy savings of the two

orientations varied between 177,572 kWh and 233,374 kWh. The use of only one DSF was found to accelerate energy loss as the transfer of heat to the interior of the building increased the amount of energy required to cool the space, resulting in an energy saving of only 1,167,520 kWh. Lastly, Scenario S00, which was the reference case study, had the worst energy savings as its high cooling demand pushed energy consumption to the upper limit of 540,919 kWh a year due to the direct exposure of all four façades to solar radiation.

7.4. General Classification of Total Energy Consumption during Cooling and Heating Periods

Lastly, the energy consumption of both the heating and cooling periods was compared. According to Table 7, Scenario S14, which used three DSFs, was the most efficient all year round as its energy consumption did not exceed 30,000 kWh. This was followed by the second group of scenarios which used either three or two DSFs, as the energy consumption ranged between 30,000 kWh and 40,000 kWh. Scenarios that utilized only one DSF were ranked third as they had energy consumptions between 40,000 kWh and 50,000 kWh. Lastly, Scenario S00, the reference case study which did not use any DSFs, was ranked last as it consumed more than 57,000 kWh of energy per year.

Table 6. General classification of energy consumption (cooling/heating).

Scenario	S0	S01	S02	S03
Yearly heating consumption KWh	37,410.61	44,651.62	34,363.02	42,293.1
Yearly cooling consumption KWh	540,919	377,464	424,199	376,333
Heating energy saving KWh	9266	2025	12,314	4384
Cooling energy saving KWh	0	163,455	116,720	164,586
Heating regime rank	13	15	12	14
Cooling regime rank	16	13	15	12
Scenario	**S04**	**S05**	**S06**	**S07**
Yearly heating consumption KWh	33,224.21	32,921.57	29,389.61	46,676.69
Yearly cooling consumption KWh	386,516	353,953	313,211	307,545
Heating energy saving KWh	13,452	13,755	17,287	0
Cooling energy saving KWh	154,403	186,966	227,708	233,374
Heating regime rank	11	10	6	16
Cooling regime rank	14	10	7	6
Scenario	**S08**	**S09**	**S10**	**S11**
Yearly heating consumption KWh	30,864.93	23,595.2	32,045.17	30,011.24
Yearly cooling consumption KWh	352,585	363,347	317,774	286,286
Heating energy saving KWh	15,812	23,081	14,632	16,665
Cooling energy saving KWh	188,334	177,572	223,145	254,633
Heating regime rank	8	4	9	7
Cooling regime rank	9	11	8	2
Scenario	**S12**	**S13**	**S14**	**S15**
Yearly heating consumption KWh	16,836.82	18,793.61	27,205.58	2217.44
Yearly cooling consumption KWh	296,572	301,022	251,845	300,031
Heating energy saving KWh	29,840	27,883	19,471	44,459
Cooling energy saving KWh	244,347	239,896	289,074	240,888
Heating regime rank	2	3	5	1
Cooling regime rank	3	5	1	4

Table 7. Final classification of energy consumption and energy saving.

Rank	1	2	3	4	5	6	7	8
Scenario	S14	S15	s12	S11	S13	S06	S10	S07
Full enrgy consumption KWh	279,051	302,249	313,410	316,298	319,816	342,601	349,819	354,222
Full energy saving KWh	299,279	276,081	264,920	262,032	258,513	235,729	228,511	224,108
Rank	9	10	11	12	13	14	15	16
Scenario	S08	S05	S09	S03	S04	S01	S02	S0
Full enrgy consumption KWh	383,450	386,875	386,943	418,626	419,740	422,116	458,563	578,330
Full energy saving KWh	194,880	191,455	191,387	159,704	158,590	156,214	119,767	0

8. Conclusions

Carefully designing the façade of a building could result in potentially significant energy savings. Double-skin façades (DSFs) are one of the most efficient methods of protecting interior environments from the effects of climate change and external environmental hazards. This present study examined the use of DSFs to improve the energy performance of high-rise office buildings in the Csa Mediterranean climate of Algiers City. The main aim of this study was to examine the performance of DSFs, especially multi-story DSFs, and the impact of two variables, namely, orientation and the number of DSFs, on the energy performance of high-rise office buildings. To that end, several models of high-rise office buildings with nine floors of an open office equipped with multi-story DSFs were created. The width of the cavity was 90 cm, with a single-glazed inner layer and double-glazed outer layer, and it ventilated naturally. The parameters of the DSF simulation model were single, juxtaposed, three, and four façades on the four main cardinal orientations. A total of 16 different scenarios were simulated using Autodesk® Ecotect® Analysis software to record the annual energy consumption during heating and cooling periods and to rank the scenarios from best to worst energy savings, as decoded and detailed in Table 8.

The primary inferences that can be drawn from the results of this present study are:

- The use of DSFs greatly benefits office buildings in a Mediterranean climate as they can provide energy savings of up to 299,279 kWh.
- The use of three DSFs was the most efficient due to a combination of the greenhouse effect and the stack effect in the cavity of the DSFs.
- The optimal DSF orientations were east, south, and west façades.
- The model with three DSFs on the east, south, and west façades reduced energy consumption in winter by 28% and 53.5% in summer.
- The use of multi-story DSFs improved the energy performance of high-rise office buildings in a Mediterranean climate by more than 250,000 kWh than buildings with no DSFs.
- The orientation of the DSFs affects their performance, while the number of DSFs used on the different façades affects the energy performance of a building.

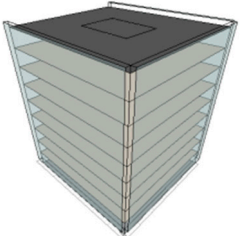**Table 8.** Decoding and final ranking of the 16 studied scenarios.

Rank	01
Code	S14
Orientation	Est-sud-ouest
Number of DSF	03

Table 8. *Cont.*
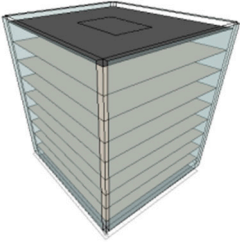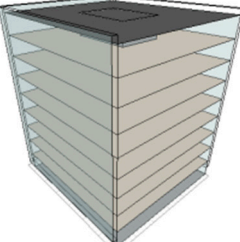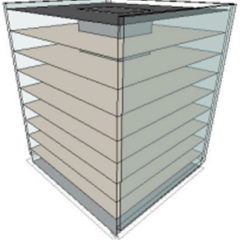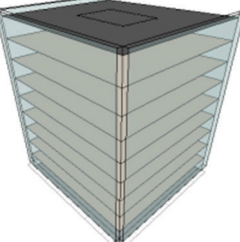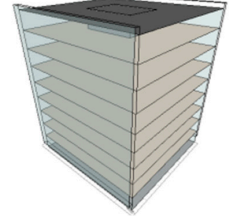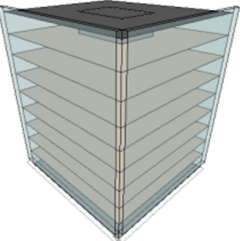
	Rank	02
	Code	S15
	Orientation	Est-sud-ouest-nord
	Number of DSF	04

	Rank	03
	Code	S12
	Orientation	Est-nord-ouest
	Number of DSF	03

	Rank	04
	Code	S11
	Orientation	Sud-est-nord
	Number of DSF	03

	Rank	05
	Code	S13
	Orientation	Nord-ouest-sud
	Number of DSF	03

	Rank	06
	Code	S06
	Orientation	Est-ouest
	Number of DSF	02

	Rank	07
	Code	S10
	Orientation	Ouest-sud
	Number of DSF	02

Table 8. *Cont.*
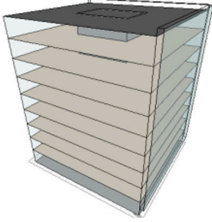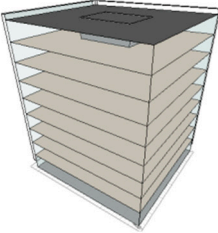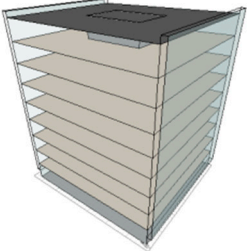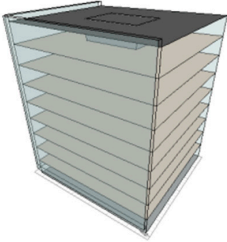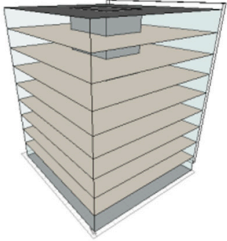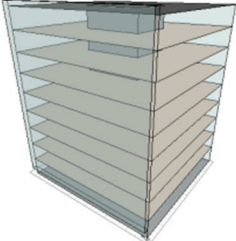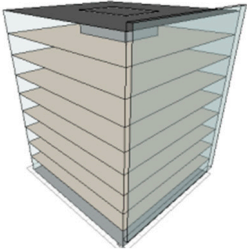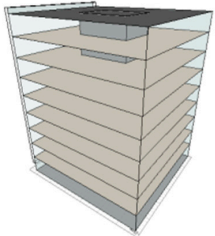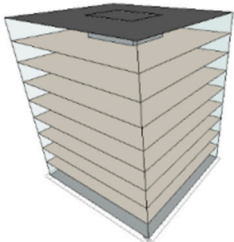
	Rank	08
	Code	S07
	Orientation	Sud-est
	Number of DSF	02

	Rank	09
	Code	S08
	Orientation	Nord-est
	Number of DSF	02

	Rank	10
	Code	S05
	Orientation	Nord-sud
	Number of DSF	02

	Rank	11
	Code	S09
	Orientation	Nord-ouest
	Number of DSF	02

	Rank	12
	Code	S03
	Orientation	EST
	Number of DSF	01

	Rank	13
	Code	S04
	Orientation	Ouest
	Number of DSF	01

Table 8. *Cont*.

	Rank	14
	Code	S01
	Orientation	Sud
	Number of DSF	01

	Rank	15
	Code	S02
	Orientation	Nord
	Number of DSF	01

	Rank	16
	Code	S0
	Orientation	/
	Number of DSF	/

References

1. Krajewska, J. The Experience of Glass Architecture—A Case Study. In Proceedings of the AHFE 2020 Virtual Conference on Human Factors in Architecture, Sustainable Urban Planning and Infrastructure, online, 16–20 July 2020; pp. 3–9.
2. Mesloub, A.; Ghosh, A. Daylighting performance of light shelf photovoltaics (LSPV) for office buildings in hot desert-like regions. *Appl. Sci.* **2020**, *10*, 7959. [CrossRef]
3. Chi, D.A.; Moreno, D.; Navarro, J. Impact of perforated solar screens on daylight availability and low energy use in offices. *Adv. Build. Energy Res.* **2021**, *15*, 117–141. [CrossRef]
4. Gorantla, K.; Shaik, S.; Kontoleon, K.J.; Mazzeo, D.; Maduru, V.R.; Shaik, S.V. Sustainable reflective triple glazing design strategies: Spectral characteristics, air-conditioning cost savings, daylight factors, and payback periods. *J. Build. Eng.* **2021**, *42*, 103089. [CrossRef]
5. Mesloub, A.; Ghosh, A.; Touahmia, M.; Albaqawy, G.A.; Alsolami, B.M.; Ahriz, A. Assessment of the overall energy performance of an SPD smart window in a hot desert climate. *Energy* **2022**, *252*, 124073. [CrossRef]
6. Nundy, S.; Mesloub, A.; Alsolami, B.M.; Ghosh, A. Electrically actuated visible and near-infrared regulating switchable smart window for energy positive building: A review. *J. Clean. Prod.* **2021**, *301*, 126854. [CrossRef]
7. Abdelhakim, M.; Lim, Y.-W.; Kandar, M.Z. Optimum glazing configurations for visual performance in Algerian classrooms under mediterranean climate. *J. Daylighting* **2019**, *6*, 11–22. [CrossRef]

8.　Mesloub, A.; Ghosh, A.; Touahmia, M.; Albaqawy, G.A.; Noaime, E.; Alsolami, B.M. Performance analysis of photovoltaic integrated shading devices (PVSDs) and semi-transparent photovoltaic (STPV) devices retrofitted to a prototype office building in a hot desert climate. *Sustainability* **2020**, *12*, 10145. [CrossRef]

9.　Ghosh, A.; Mesloub, A.; Touahmia, M.; Ajmi, M. Visual Comfort Analysis of Semi-Transparent Perovskite Based Building Integrated Photovoltaic Window for Hot Desert Climate (Riyadh, Saudi Arabia). *Energies* **2021**, *14*, 1043. [CrossRef]

10.　Zhang, Y.; Zhang, Y.; Li, Z. A novel productive double skin façades for residential buildings: Concept, design and daylighting performance investigation. *Build. Environ.* **2022**, *212*, 108817. [CrossRef]

11.　Lucchino, E.C.; Gelesz, A.; Skeie, K.; Gennaro, G.; Reith, A.; Serra, V.; Goia, F. Modelling double skin façades (DSFs) in whole-building energy simulation tools: Validation and inter-software comparison of a mechanically ventilated single-story DSF. *Build. Environ.* **2021**, *199*, 107906. [CrossRef]

12.　Bonham, M.B. *Bioclimatic Double-Skin Façades*; Routledge: Oxfordshire, UK, 2019.

13.　Poirazis, H. *Double Skin Façades for Office Buildings*; Report EBD; Lund University: Lund, Sweden, 2004.

14.　Djeffal, L. *The Double Skin Façade as a Support Tool for Improving the Energy Performance of a Building in a Mediterranean Climate, Case of Study: Algiers Multifunctional Center*; Larbi Tebessi University: Tebessa, Algaria, 2019.

15.　Wang, M.; Hou, J.; Hu, Z.; He, W.; Yu, H. Optimisation of the double skin facade in hot and humid climates through altering the design parameter combinations. *Build. Simul.* **2021**, *14*, 511–521. [CrossRef]

16.　Preet, S.; Sharma, M.K.; Mathur, J.; Chowdhury, A.; Mathur, S. Performance evaluation of photovoltaic double-skin facade with forced ventilation in the composite climate. *J. Build. Eng.* **2020**, *32*, 101733. [CrossRef]

17.　Matour, S.; Hansen, V.; Hansen, R.; Drogemuller, R.; Omran, S. Adaptation of Double Skin Facade for warm climate from a wind harvesting perspective in tall buildings. In Proceedings of the 53rd International Conference of the Architectural Science Association 2019, Roorkee, India, 28–30 November 2019.

18.　Mayer, N. Climat méditerranéen. Available online: https://www.futura-sciences.com/planete/definitions/climatologie-climat-mediterraneen-16806/ (accessed on 20 March 2022).

19.　Yellamraju, V. Evaluation and Design of Double-Skin Facades for Office Buildings in Hot Climates. Master's Thesis, Texas A&M University, College Station, TX, USA, 2004.

20.　Saelens, D. *Energy Performance Assessment of Single Storey Multiple-Skin Facades*; Katholieke Universiteit Leuven: Leuven, Belgium, 2002.

21.　Mulyadi, R. *Study on Naturally Ventilated Double-Skin Facade in Hot and Humid Climate*; Nagoya University: Aichi, Japan, 2012.

22.　Azarbayjani, M. *Beyond Arrows: Energy Performance of a New, Naturally Ventilated, Double-Skin Facade Configuration for a High-Rise Office Building in Chicago*; University of Illinois at Urbana-Champaign: Urbana, IL, USA, 2010.

23.　Barbosa, S.; Ip, K.J.R.; Reviews, S.E. Perspectives of double skin façades for naturally ventilated buildings: A review. *Renew. Sustain. Energy Rev.* **2014**, *40*, 1019. [CrossRef]

24.　Barbosa, S.; Ip, K.; Southall, R. Influence of key site parameters on the thermal performance of double skin facades in naturally ventilated buildings in a tropical climate. In Proceedings of the 31st International PLEA Conference: Architecture in (r)evolution, Bologna, Italy, 9–11 September 2015.

25.　Souza, E. How Do Double-Skin Façades Work? Available online: https://www.archdaily.com/922897/how-do-double-skin-facades-work (accessed on 20 March 2022).

26.　Yoon, N.; Min, D.; Heo, Y. Dynamic compartmentalization of double-skin façade for an office building with single-sided ventilation. *Build. Environ.* **2022**, *208*, 108624. [CrossRef]

27.　Hong, X.; Lin, J.; Yang, X.; Wang, S.; Shi, F. Comparative Analysis of the Daylight and Building-Energy Performance of a Double-Skin Facade System with Multisectional Shading Devices of Different Control Strategies. *J. Energy Eng.* **2022**, *148*, 05022001. [CrossRef]

28.　Radhi, H.; Sharples, S.; Fikiry, F. Will multi-facade systems reduce cooling energy in fully glazed buildings? A scoping study of UAE buildings. *Energy Build.* **2013**, *56*, 179–188. [CrossRef]

29.　Chan, A.; Chow, T.T.; Fong, K.; Lin, Z. Investigation on energy performance of double skin façade in Hong Kong. *Energy Build.* **2009**, *41*, 1135–1142. [CrossRef]

30.　Guardo, A.; Coussirat, M.; Egusquiza, E.; Alavedra, P.; Castilla, R. A CFD approach to evaluate the influence of construction and operation parameters on the performance of Active Transparent Façades in Mediterranean climates. *Energy Build.* **2009**, *41*, 534–542. [CrossRef]

31.　Haase, M.; Amato, A. An investigation of the potential for natural ventilation and building orientation to achieve thermal comfort in warm and humid climates. *Sol. Energy* **2009**, *83*, 389–399. [CrossRef]

32.　Tao, Y.; Zhang, H.; Zhang, L.; Zhang, G.; Tu, J.; Shi, L. Ventilation performance of a naturally ventilated double-skin façade in buildings. *Renew. Energy* **2021**, *167*, 184–198. [CrossRef]

33.　Pappas, A.; Zhai, Z. Numerical investigation on thermal performance and correlations of double skin façade with buoyancy-driven airflow. *Energy Build.* **2008**, *40*, 466–475. [CrossRef]

34.　Yoon, Y.B.; Seo, B.; Koh, B.B.; Cho, S. Heating energy savings potential from retrofitting old apartments with an advanced double-skin façade system in cold climate. *Front. Energy* **2020**, *14*, 224–240. [CrossRef]

35.　Gratia, E.; De Herde, A. The most efficient position of shading devices in a double-skin facade. *Energy Build.* **2007**, *39*, 364–373. [CrossRef]

36. Shakouri, M.; Ghadamian, H.; Noorpoor, A. Quasi-dynamic energy performance analysis of building integrated photovoltaic thermal double skin façade for middle eastern climate case. *Appl. Therm. Eng.* **2020**, *179*, 115724. [CrossRef]

37. Ahriz, A.; Mesloub, A.; Elkhayat, K.; Alghaseb, M.A.; Abdelhafez, M.H.; Ghosh, A. Development of a Mosque Design for a Hot, Dry Climate Based on a Holistic Bioclimatic Vision. *Sustainability* **2021**, *13*, 6254. [CrossRef]

38. Chaudhry, A.A.; Buchwald, J.; Nagel, T. Local and global spatio-temporal sensitivity analysis of thermal consolidation around a point heat source. *Int. J. Rock Mech. Min. Sci.* **2021**, *139*, 104662. [CrossRef]

39. Tian, W. A review of sensitivity analysis methods in building energy analysis. *Renew. Sustain. Energy Rev.* **2013**, *20*, 411–419. [CrossRef]

40. Google_Earth. Algiers. Available online: https://earth.google.com/web/@28.02895485,1.66619395,547.24213155a,5253216.414 44454d,35y,0h,0t,0r/data=Cl0aWxJVCiQweGQ3ZThhNmEyODAzN2JkMToweDcxNDBiZWUzYWJkN2Y4YTIZ0cq9wKwIP EAh8nUZ_tON-j8qG-C5geC4reC4peC4iOC4teC5gOC4o-C4teC4ohgCIAE (accessed on 21 March 2022).

41. Kottek, M.; Grieser, J.; Beck, C.; Rudolf, B.; Rubel, F. World map of the Köppen-Geiger climate classification updated. *Meteorol. Zeitschrif* **2006**, *15*, 259–263. [CrossRef]

42. METEONORM. *Global Meteorological Database*; METEOTEST Genoss: Bern, Switzerland, 2021.

43. Climats-Du-Monde. Climat-Algerie. Available online: https://www.climatsetvoyages.com/climat/algerie (accessed on 20 March 2022).

44. Spark, W. Climate and Average Weather Year Round in Algiers. Available online: https://weatherspark.com/y/48929/Average -Weather-in-Algiers-Algeria-Year-Round (accessed on 31 January 2022).

45. Musdinar, I.; Ardli, R.A. Performance evaluation of sub ground passive cooling system with Ecotech software simulation (Case study: Pasio Christi Church at Cibunut, Kuningan, West Java). *IOP Conf. Ser. Earth Environ. Sci.* **2021**, *878*, 012006. [CrossRef]

46. Hermawan, S.; Kholil, A. The analysis of thermal performance of vernacular building envelopes in tropical high lands using Ecotect. *IOP Conf. Ser. Earth Environ. Sci.* **2020**, *423*, 012004. [CrossRef]

47. Senthilkumar, K.; Taj, G. Design of Energy Efficient Educational Institutional Building. In *Recent Developments in Sustainable Infrastructure (ICRDSI-2020)—Structure and Construction Management: Conference Proceedings from ICRDSI-2020 Volume 1*; Das, B.B., Gomez, C.P., Mohapatra, B.G., Eds.; Springer Nature Singapore: Singapore, 2022; pp. 677–691. [CrossRef]

48. Zhang, Y. *Study on Energy-Saving Thermal Environment of Residential Envelope Reconstruction Based on ECOTECT*; SPIE: Washington, DC, USA, 2021; Volume 12050.

49. Sadat, N. Assessing Thermal Performance of Mud House Using ECOTECT Analysis—A Case of Vernacular Architecture in Northern Bangladesh. *Am. Acad. Sci. Res. J. Eng. Technol. Sci.* **2021**, *79*, 79–87.

50. Aboud, N. Analysis on thermal performance for increasing energy efficiency: A case study for Tripoli-Libya, using Ecotect®. *Sol. Energy Sustain. Dev.* **2021**, *10*, 20–33. [CrossRef]

51. Soufiane, F.; Atef, A.; Mohamed, M.; Salaheddine, D. Quantifying the effectiveness of mass proportions and the orientation for buildings on thermal performance in Tebessa, Algeria. *IOP Conf. Ser. Earth Environ. Sci.* **2019**, *397*, 012008. [CrossRef]